IEEE Access
Multidisciplinary | Rapid Review | Open Access Journal

Received March 25, 2020, accepted April 3, 2020, date of publication April 9, 2020, date of current version April 27, 2020.

Digital Object Identifier 10.1109/ACCESS.2020.2986763

Design of a 7-Way Microstrip Divider for a Hexagonal Honeycomb Structure

EUIBUM LEE, (Student Member, IEEE), AND HYUNCHUL KU, (Member, IEEE)
Department of Electronic Engineering, Konkuk University, Seoul 05029, South Korea

Corresponding author: Hyunchul Ku (hcku@konkuk.ac.kr)

This work was supported in part by the Basic Science Research Program through the National Research Foundation of Korea (NRF) funded by the Ministry of Education under Grant NRF-2017R1D1A1B03032927, and in part by the NRF Grant funded by the Korean Government (MSIP) under Grant NRF-2017R1A5A1015596.

ABSTRACT This paper proposes a 7-way microstrip divider for hexagonal honeycomb structures. The honeycomb arrangement has advantages such as equidistant adjacent output ports and high space utilization. The structure comprises six output ports arranged hexagonally and one output port placed at the center of the hexagon in the same plane. To design such a divider considering the output ports' positions, this paper proposes the combination of a microstrip 6:1 unequal Wilkinson divider and a 6-way microstrip divider. To facilitate the implementation of the 6:1 unequal divider, including a transmission line with a high characteristic impedance, a microstrip coupler is used, and for the 6-way microstrip divider, a design scheme and analysis considering the impedance matching and isolation of the output ports are presented. Moreover, the ground layers of the two microstrip dividers are constructed in a back-to-back structure to minimize the size of the overall divider. For validation, a 5.8 GHz 7-way divider is designed, implemented, and measured. The measured S-parameters show that the proposed 7-way divider has appropriate return loss, insertion loss, isolation, and power distribution with a phase difference under 4.7°.

INDEX TERMS Microwave circuit, power divider, microstrip, 7-way divider, hexagonal honeycomb.

I. INTRODUCTION

Advanced microwave technologies, such as a phased array antenna are being employed not only in military radars but also in most wireless systems (communications [1], [2], wireless power charging [3]). A phased array antenna, depending on the arrangement of the elements, has different synthesized beam properties, and consequently, respective advantages and disadvantages [4]. Among the various arrangements, the hexagonal lattice arrangement has excellent advantages, such as optimum structural space utilization and few grating lobes, because all the adjacent antenna elements can be placed equidistantly [4]. To implement such an array structure, it is important to divide the microwave signal into n-ways by appropriately considering the location of the output ports.

Various studies have been conducted on n-way dividers [5]–[11]. An n-way divider can be implemented in two representative forms: a tree structure in which a reference signal is divided gradually through consecutive trees [5], [6] or, a scattering structure in which a reference signal is directly divided into n-ways [7], [8]. A tree structure divider requires a relatively large amount of space because it contains consecutive dividers connected up to n-way, while a scattering structure divider cannot easily accommodate one output port at the center of other output ports. Due to these issues, designers find it difficult to implement a space-efficient divider with a single scheme. To overcome these difficulties, we propose a novel method to design a 7-way divider that helps facilitate applications involving hexagonal honeycomb structures.

In the proposed design, a 6:1 unequal divider is combined with a 6-way scattering structure divider in the form of a consecutive tree [12] and a back-to-back microstrip structure for miniaturization [13]. However, a problem with the 6:1 unequal divider design is that one of the impedance transforming transmission lines (ITTLs) theoretically requires a considerably high characteristic impedance value. Moreover, even if an ITTL with a high characteristic impedance can be fabricated using an ordinary method, its electrical properties will not match the mathematically calculated values [14]. Various alternatives have been proposed, such as using a

The associate editor coordinating the review of this manuscript and approving it for publication was Chow-Yen-Desmond Sim.

This work is licensed under a Creative Commons Attribution 4.0 License. For more information, see https://creativecommons.org/licenses/by/4.0/

defected ground structure (DGS) [15], [16] or a co-planar waveguide with an electronic bandgap (EBG CPW) [17], [18]. However, these have several drawbacks, such as requiring processes on the ground layer and a sufficient air gap (distance) from other conductors. To overcome these problems, the unequal divider requires other methods for implementing the space-efficient back-to-back structure. Furthermore, as previously reported dividers with scattering structures [7], [8] are also inappropriate for a planar back-to-back structure considering the arrangement of the resistors in [7] or the waveguide structure in [8], a new design method is desired for the scattering structure divider as well. We propose a novel design method for each divider. First, a microstrip unequal divider with a loosely coupled microstrip line coupler is proposed to avoid the problem of high characteristic impedance. We provide a mathematically analyzed design solution that uses ring-arrangement resistors for isolation and impedance matching for the 6-way microstrip scattering structure divider. Consequently, the two proposed dividers can be combined into a 7-way divider in a back-to-back structure. As a result, the proposed 7-way divider can be used for applications involving hexagonal honeycomb structures.

The rest of this paper is organized as follows. Section II presents the designs and analyses of the 6:1 uneven Wilkinson divider, 6-way scattering structure divider, and 7-way divider which is a combination of the two dividers. Section III discusses the implementation of the proposed divider and its performance with simulated and measured results. Finally, Section IV presents the conclusions of this study.

II. DESIGN OF THE 7-WAY DIVIDER

Fig. 1 shows an example of a system with a hexagonal honeycomb structure. In this system, the seven antennae and the active microwave module are arranged equidistantly in the form of a hexagonal honeycomb.

To implement such a system, a 7-way divider is necessary. In this section, the design and analysis of the proposed 7-way divider is described. Before describing the detailed process, a brief guideline of the design process is given as follows.

1) Design and analyze the 6:1 unequal Wilkinson divider to divide the input power with a 6:1 ratio
2) Design and analyze a high impedance ITTL in the divider using a microstrip line coupler
3) Design and analyze a ring-type 6-way scattering structure divider
4) Determine the resistance between the output ports of the 6-way divider considering the output impedance and isolation
5) Combine the unequal Wilkinson divider and the 6-way scattering structure divider in back-to-back structure
6) Adjust the parameters and analyze the frequency responses of the divider by the performing a full-wave simulation

Steps 1 & 2 are described in section II-A, steps 3 & 4 in section II-B, step 5 in section II-C, and step 6 in Section III.

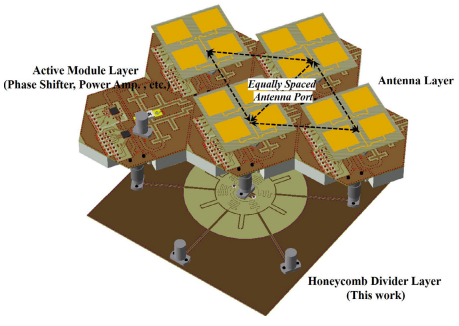

FIGURE 1. Hexagonal honeycomb array antenna module.

A. 6:1 UNEQUAL WILKINSON POWER DIVIDER

Fig. 2 depicts a schematic of the N:1 unequal Wilkinson divider comprising several quarter-wavelength ITTLs. The power ratio (K) follows $\sqrt{P_B/P_A}$, where P_A and P_B are respectively the output power at Ports A and B, and its design values are obtained using the following equations [12]. In this section, analyses are made on the target frequency (f_0), and the frequency responses of the designed divider are investigated through a full-wave simulation described in the next section.

$$Z_1 = Z_0\sqrt{K(1+K^2)} \tag{1a}$$

$$Z_2 = Z_0\sqrt{\frac{1+K^2}{K^3}} \tag{1b}$$

$$Z_3 = \sqrt{Z_0{}^2K} \tag{1c}$$

$$Z_4 = \sqrt{Z_0{}^2/K} \tag{1d}$$

$$R_x = Z_0(K + \frac{1}{K}) \tag{1e}$$

The variables used in (1) are described in Fig. 2. Z_n ($n = 1, 2, 3, 4$) is the characteristic impedance of the transmission line, and θ_n ($n = 1, 2, 3, 4$) is the electrical length of the transmission line for the given frequency. When the in/output port impedance is set to Z_0, every characteristic impedance of the ITTL needs to be set based on the results of (1). If the output power ratio (K) is set to $\sqrt{6}$, Z_1 must be approximately $4.14Z_0$; therefore, a loosely coupled microstrip line coupler, which is available on a uni-surface, is adopted to replace Z_1. Fig. 3(a) depicts such a microstrip coupler [19], comprising two ports with two other diagonal ports being shorted. Y in (2)

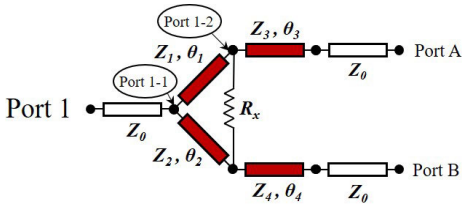

FIGURE 2. Schematic of N:1 unequal Wilkinson power divider.

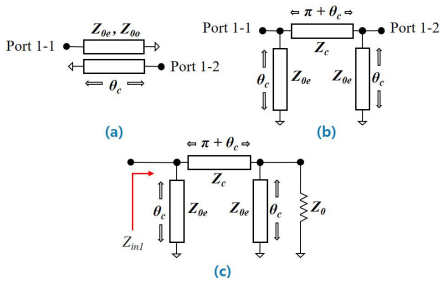

FIGURE 3. (a) Microstrip coupler with two diagonal two ports shorted and (b) Equivalent circuit of Fig. 3(a), and (c) Input impedance of the circuit depicted in Fig. 3(b) terminated with Z_0.

is the admittance matrix of the coupler depicted in Fig. 3(a).

$$[Y] = -jY_{0e}\cot\theta_c \begin{bmatrix} 1 & 0 \\ 0 & 1 \end{bmatrix} + j\frac{Y_{0o} - Y_{0e}}{2} \begin{bmatrix} -\cot(\pi+\theta_c) & \csc(\pi+\theta_c) \\ \csc(\pi+\theta_c) & -\cot(\pi+\theta_c) \end{bmatrix} \quad (2)$$

Combining (2) and the structure shown in Fig. 3(a) results in a model equivalent to a double stub, as depicted in Fig. 3(b) [20]. Z_{0e} and Z_{0o} are the even- and odd mode impedances of the transmission line coupler, and Y_{0e} and Y_{0o} are their inverses, respectively. The first term in (2) is identical to the two short stubs with a characteristic impedance of Z_{0e} and the second term with a $(\pi + \theta_c)$ length of transmission line with characteristic impedance $Z_c = [(Y_{0o} - Y_{0e})/2]^{-1}$. The conventional even- and odd-mode impedances using a coupling coefficient (C) gives the equation for Z_c [21].

$$Z_{0e} = Z_0\sqrt{\frac{1+C}{1-C}} \quad (3a)$$

$$Z_{0o} = Z_0\sqrt{\frac{1-C}{1+C}} \quad (3b)$$

$$Z_c = \left(\frac{Y_{0o} - Y_{0e}}{2}\right)^{-1} = Z_0\sqrt{\frac{1}{C^2} - 1} \quad (3c)$$

Given that one of the ports in Fig. 3(b) is terminated with Z_0, as depicted in Fig. 3(c), an equation for the input impedance (Z_{in1}) is obtained below.

$$Z_{in1} = [-jY_{0e}\cot\theta_c + Y_c\frac{-jY_{0e}\cot\theta_c + Y_0 + jY_c\tan\theta_c}{Y_c + j(-jY_{0e}\cot\theta_c + Y_0)\tan\theta_c}]^{-1} \quad (4)$$

Here, Y_c is Z_c^{-1} and Y_0 is Z_0^{-1}. For $\theta_c = \pi/2$, (4) can be simplified as follows.

$$Z_{in1} = \frac{Z_c^2}{Z_0} \quad (5)$$

Here, (5) indicates that the input impedance (Z_{in1}) is equivalent to a $3\pi/2$ ITTL with a characteristic impedance of Z_c theoretically. Therefore, it implies that the characteristic impedance of Z_1 can be replaced with Z_c by adjusting the transmission line coupler, whose parameters are Z_{0e} and Z_{0o}. Once the issue of the characteristic impedance of Z_1 is solved, the other characteristic impedance values from (1) are easily available. However, as depicted in Fig. 3, as the $\pi/2$ length of the transmission line coupler is consistent with $3\pi/2$ length of the transmission line with a characteristic impedance of Z_c (Z_1), the length of the transmission line with Z_2 should also be matched for the same phase delay.

B. PROPOSED 6-WAY MICROSTRIP SCATTERING STRUCTURE DIVIDER

When an n-way scattering structure divider is fabricated with a junction resistor node [7] or by using a waveguide format [8], the design provides good output port impedance and isolation between all the output ports. However, this is not implementable with an ordinary planar microstrip line. Therefore, we propose a planar ring resistor arrangement for output impedance matching and isolation as depicted in Fig. 4.

The arrangement in Fig. 4 consists of several ITTLs whose characteristic impedance is Z_α or Z_β. The Z_β value and length are important to apply the resistors (R_y) without any impedance distortion. However, the length of the line with Z_β is assumed to be 0 to obtain an adequate R_y value first. Every port in Fig. 4 other than Port 2 is terminated with Z_0, and an arbitrary source (V_s) is applied to Port 2, as depicted in Fig. 5.

The characteristic impedance Z_α is $\sqrt{6Z_0^2}$ [12], and by applying a transmission line equation when the physical length of every transmission line of Z_α is set to $\lambda/4$, we can obtain the correlations between the node voltages

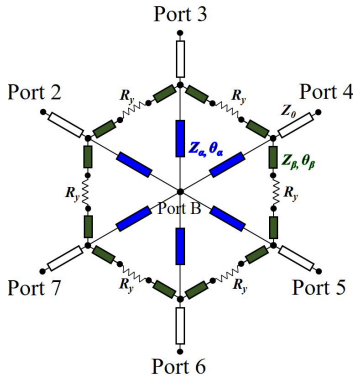

FIGURE 4. Schematic of a 6-way microstrip scattering structure divider.

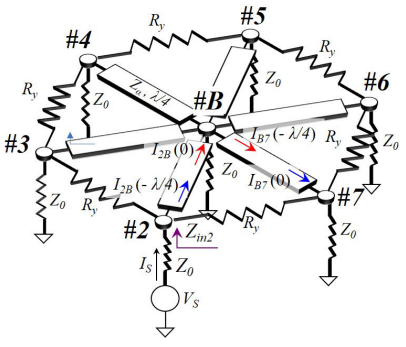

FIGURE 5. Microstrip scattering structure divider with Z_0 termination.

V_n $(n = 2, 3, \ldots, 7)$ and center node voltage V_B as follows:

$$V(z) = (V_\alpha^+ + V_\alpha^-)\cos kz + j(V_\alpha^+ - V_\alpha^-)\sin kz \quad (6a)$$
$$V(0) = (V_\alpha^+ + V_\alpha^-) = V_B \quad (6b)$$
$$V(-\lambda/4) = j(V_\alpha^+ - V_\alpha^-) = V_n \quad (6c)$$

In (6), V_α^+ and V_α^- are the wave voltages in the ITTL whose characteristic impedance is Z_α, and k is the wave-number which is $2\pi/\lambda$ under lossless conditions. Additional simultaneous equations can be obtained as follows:

$$I_{nB}(z) = \frac{j}{Z_\alpha}(V_\alpha^+ - V_\alpha^-)\cos kz + \frac{j}{Z_\alpha}(V_\alpha^+ + V_\alpha^-)\sin kz \quad (7a)$$
$$I_{nB}(0) = \frac{j}{Z_\alpha}(V_\alpha^+ - V_\alpha^-) = \frac{jV_n}{Z_\alpha} \quad (7b)$$
$$I_{nB}(-\lambda/4) = \frac{j}{Z_\alpha}(V_\alpha^+ + V_\alpha^-) = \frac{jV_B}{Z_\alpha} \quad (7c)$$

The current flowing from node #n to #B, I_{nB}, and that in the opposite direction, I_{Bn}, can also be obtained in (7). A matrix-vector equation between the node voltages and source voltage can be obtained in the form of (8), as shown at the bottom of the next page, using the Kirchhoff current law (KCL). The input impedance (Z_{in2} shown in Fig. 5) is the ratio of the voltage at node #2 to the current I_s generated from V_s, and the isolation becomes perfect when the magnitude of the applied voltage at every node except #2 and #B becomes zero. Z_{in2} and isolation are simultaneous dependent variables of the resistance R_y, as depicted in Figs. 6 and 7 respectively.

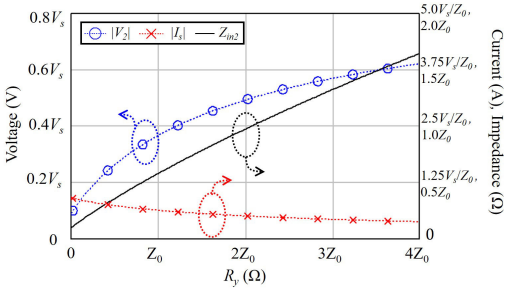

FIGURE 6. V_2, I_S and Z_{in2} vs R_y.

Fig. 6 shows that Z_{in2} is closest to Z_0 when R_y is approximately $2.08Z_0$. Fig. 7 shows that there is no specific resistance value that makes the voltage applied to every node except #2 and #B be zero. Thus, R_y is selected as $2.08Z_0$ such that every node voltage except V_2 and V_B are close to zero on average

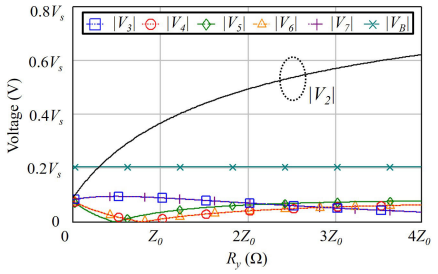

FIGURE 7. Voltage magnitude at node #n (V_n) vs R_y.

and highly satisfies the output impedance matching, which affects the stability of the circuit.

As mentioned previously, additional transmission lines (Z_β, θ_β) should be considered to connect the resistor (R_y), because its arbitrary value causes severe in/out impedance distortion owing to the extremely short wavelength of approximately a few centimeters. Fig. 8 depicts the in/output port reflection with Z_β and θ_β.

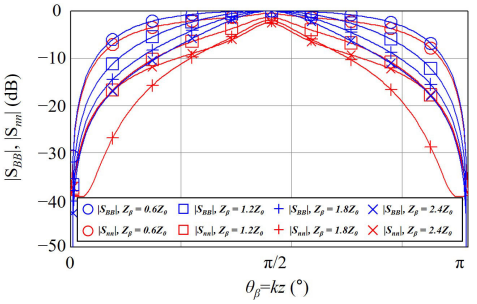

FIGURE 8. In (S_{BB})/output (S_{nn}) port reflection for Z_β and θ_β variation ($n = 2, 3, \ldots, 7$).

As depicted in Fig. 8, when θ_β is $\pi/2$, it results in the worst reflection at the input (S_{BB}) and output (S_{nn}) ports $(n = 2, 3, \ldots, 7)$, whereas when it is 0 or π, it results in the best reflection. Furthermore, the best overall reflection is when the characteristic impedance of Z_β is approximately $1.8\,Z_0$. Moreover, because, the length θ_β is not available with zero, the θ_β should be π.

C. PROPOSED 7-WAY DIVIDER

The next step is to design a 7-way divider by combining the two dividers designed in the previous Section II-A and B. Fig. 9 depicts a schematic of the proposed 7-way divider.

$$\begin{bmatrix} R_y+2Z_0 & -Z_0 & 0 & 0 & 0 & -Z_0 & j(R_yZ_0/Z_\alpha) \\ -Z_0 & R_y+2Z_0 & -Z_0 & 0 & 0 & 0 & j(R_yZ_0/Z_\alpha) \\ 0 & -Z_0 & R_y+2Z_0 & -Z_0 & 0 & 0 & j(R_yZ_0/Z_\alpha) \\ 0 & 0 & -Z_0 & R_y+2Z_0 & -Z_0 & 0 & j(R_yZ_0/Z_\alpha) \\ 0 & 0 & 0 & -Z_0 & R_y+2Z_0 & -Z_0 & j(R_yZ_0/Z_\alpha) \\ -Z_0 & 0 & 0 & 0 & -Z_0 & R_y+2Z_0 & j(R_yZ_0/Z_\alpha) \\ j/Z_\alpha & j/Z_\alpha & j/Z_\alpha & j/Z_\alpha & j/Z_\alpha & j/Z_\alpha & 1/Z_0 \end{bmatrix} \begin{bmatrix} V_2 \\ V_3 \\ V_4 \\ V_5 \\ V_6 \\ V_7 \\ V_B \end{bmatrix} = \begin{bmatrix} R_yV_s \\ 0 \\ 0 \\ 0 \\ 0 \\ 0 \\ 0 \end{bmatrix} \quad (8)$$

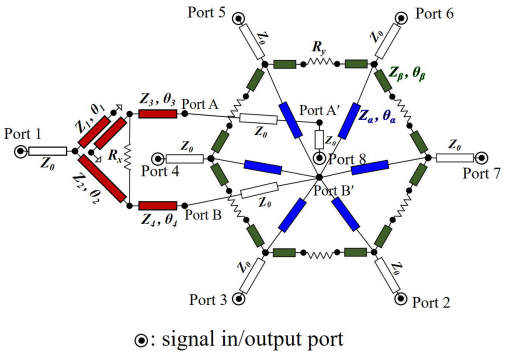

FIGURE 9. Schematic of proposed 7-way divider.

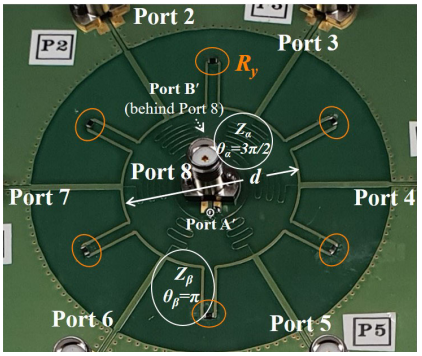

FIGURE 10. Fabricated 7-way divider and output port arrangement. (*d* is the diameter of the ring).

As shown in Fig. 9, the output port A of the unequal Wilkinson divider is connected to Port A′ which supplies the smaller portion of the divided power to Port 8, and the output port B to Port B′ directly supplies the larger portion to the scattering structure divider. The length of the transmission lines with Z_0 impedance in Fig. 9 can be adjusted considering the phase of the output signal and the size of the divider. From the previous subsections A and B, the parameters of the transmission line (Z_n, θ_n) and resistors (R_x, R_y) used in each divider can be acquired, and summarized in Table 1.

TABLE 1. Derived design values of 7-way divider.

Z_1	Z_{0e}	1.27 Z_0	θ_1	$\pi/2$
	Z_{0o}	0.79 Z_0		
Z_2		0.69 Z_0	θ_2	$3\pi/2$
Z_3		1.57 Z_0	θ_3	$\pi/2$
Z_4		0.64 Z_0	θ_4	$\pi/2$
Z_α		2.45 Z_0	θ_α	$\pi/2$
Z_β		1.80 Z_0	θ_β	π
R_x		2.86 Z_0	R_y	2.08 Z_0

In the next section, we describe the implementation of the proposed 7-way divider and its performance. Unlike other *n*-way dividers [7], [8], [15]–[18], the two designed microstrip dividers contain an intact ground surface and have an appropriate shape to realize the back-to-back combination. To minimize the size of the 7-way divider, two dividers are constructed in a back-to-back structure.

III. FABRICATIONS AND VERIFICATION

Based on the theoretical values obtained in the previous section, the two dividers are fabricated and combined in this section. The network impedance (Z_0) is set to 50Ω, and the target frequency is set to 5.8 GHz. Arlon TC-350 ($\epsilon_r = 3.5$, 20 mil, 1 oz) is used as a microstrip line substrate.

To implement the 7-way divider with a honeycomb structure, the seven output ports need to be placed at the center and six vertices of the hexagon. Thus, one output port is added at the center of the 6-way scattering structure divider as shown in Fig. 10, and it is connected to the output port A of the unequal Wilkinson divider by a ground etched via hole method which minimizes impedance distortions [22]. The additional output port 8 is at the center of the ring; thus, the input port of the 6-way scattering structure divider (Port B′) is located slightly off-center and is also connected using the ground etched via hole method [22]. Considering the size of the divider and location of the output ports in this example, the electrical length (θ_α) of the Z_α transmission line is adjusted to $3\pi/2$ ($\theta_\alpha = \pi + \pi/2$) and the Z_α, Z_β transmission lines were implemented in a bent form, as shown in Fig. 10.

To verify the performance of the seven outputs, shown in Fig. 10, we conduct a full-wave simulation using an EM simulator (AWR Axiem from Cadence). Fig. 11(a) and (b) show the layout for EM simulation and frequency response. The circuit shown in Fig. 10 has two inputs, one of which is the input of the scattering structure divider (Port B) and the other is the input (Port A) via through from an output of the unequal Wilkinson divider. Fig. 11(b) shows the measured frequency response of $|S_{nB'}|$ ($n = 2, 3, \ldots, 7$) for the fabricated 6-way divider and the center via through, $|S_{8A'}|$. A vector network analyzer P5007A (Agilent) is used for measurement. The simulation results using Fig. 11(a) are largely in agreement with the measured

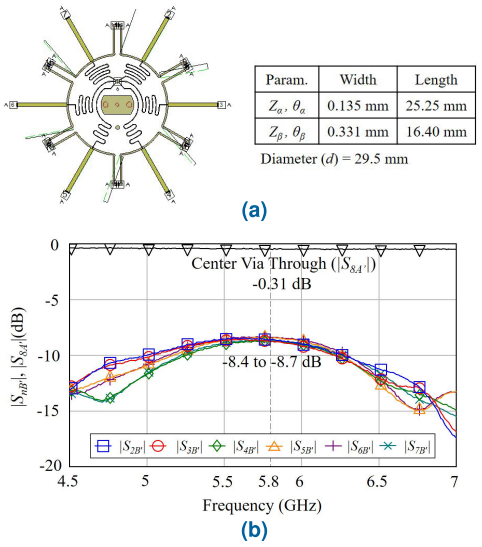

FIGURE 11. (a) Layout for EM-simulation and (b) Measured frequency response of two types paths.

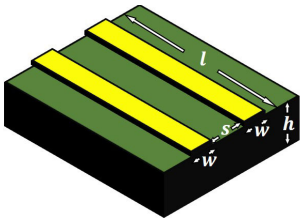

w	0.945 mm
l	7.95 mm
s	0.195 mm
h	0.5 mm

TC-350, Arlon
(ϵ_r = 3.5, 1 oz)

FIGURE 12. Parameters of the microstrip coupler for Z_1.

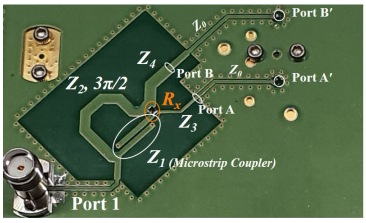

Param.	Width	Length
Z_1, θ_1	Presented in Fig. 12	
Z_2, θ_2	1.92 mm	7.61 mm
Z_3, θ_3	0.46 mm	8.11 mm
Z_4, θ_4	2.13 mm	7.57 mm

FIGURE 13. Fabricated 6:1 unequal divider using microstrip coupler.

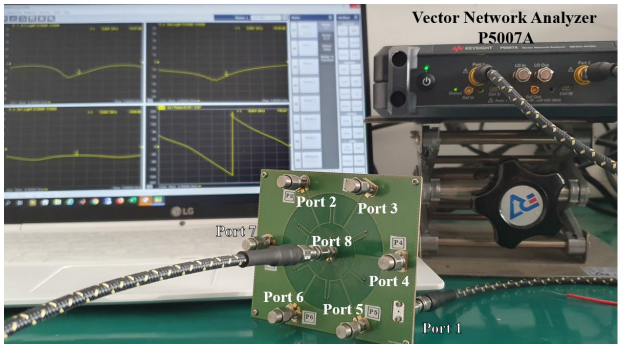

FIGURE 14. Fabricated 7-way microstrip divider under test.

results; therefore, only the measured results are presented. Because all the seven output ports of the proposed divider need to supply equally distributed power from the source, the frequency response, shown in Fig. 11(b) must be reflected in the design of the uneven Wilkinson divider. As depicted in Fig. 11(b), the measured frequency response of $|S_{nB'}|$ includes an additional insertion loss of approximately 0.8 dB in comparison with the theoretical 6-way divider (7.78 dB), and the center via through frequency response of ($|S_{8A'}|$) has an insertion loss of approximately 0.3 dB. Thus, the ratio of the unequal divider is adjusted to 6.8:1 for equal power distribution. When the characteristic impedance is calculated with a power ratio of 6.8:1 using (1), the highest characteristic value Z_1 is approximately 225.5 Ω. It is replaced with $Z_{0e} =$ 62.33 Ω and $Z_{0o} = 40.11$ Ω using (3). A microstrip coupler that satisfies these conditions is determined using the AWR Axiem; Fig. 12 depicts the coupler line converted from a high impedance line and its physical values.

The extracted characteristic impedances of the remaining microstrip lines for the unequal Wilkinson divider are $Z_2 = 33.16$ Ω, $Z_3 = 80.74$ Ω, and $Z_4 = 30.96$ Ω respectively. A microstrip line with these impedances can be easily implemented with the conventional method. Fig. 13 shows the fabricated unequal Wilkinson divider and its parameters.

The proposed 7-way divider is fabricated by connecting the two implemented dividers back-to-back; Fig. 14 depicts the fabricated 7-way honeycomb structure divider and its test environment.

Fig. 15 depicts the measured results of the frequency response; the order of the port numbers is the same as that depicted in Fig. 9. To verify the key indicators of the divider, such as the insertion loss, phase delay, reflection, and isolation, the measurements are compared with the full-wave simulation using AWR Axiem. First, to validate the insertion loss and phase of each output port, the magnitude, and phase of S_{n1} ($n = 2, 3, \ldots, 8$) are plotted in Figs. 15(a) and (b), respectively. To validate the reflection loss of the divider, S_{nn} ($n = 1, 2, \ldots, 8$) are plotted in Fig. 15(c), and finally, to check the isolation of the divider, that highly affects the stability of the circuit, we provide S_{2n} ($n = 3, 4, \ldots, 8$) in Fig. 15(d). Because the isolation between the other ports is measured similarly, only S_{2n} is presented in the figure. As a result, the four indicators of the proposed divider, namely the insertion loss, phase difference, reflection loss, and isolation, are 9.3 - 9.7 dB, under 4.7°, >16 dB and >18 dB at the target frequency of 5.8 GHz, respectively, The results are in good agreement with the simulation results.

Finally, the proposed divider is compared with several n-way dividers [6], [9]–[11] as listed in Table 2.

TABLE 2. Comparison with other works.

	[6]	[9]	[10]	[11]	**This Work**
# of Output Port	4	5	9	4	**7**
Substrate Structure	Single Microstrip	Single Microstrip	Single Microstrip With Graphene Flake	Double Microstrip (SIW Slot Coupling)	**Double Microstrip (Back to Back)**
Freq. Band (BW)	L-Band (10 %)	C-Band (21 %)	L-band (38 %)	X-band (18 %)	**C-band (15 %)**
Average IL	6.5 dB	7.3 dB	10.5 dB	7.6 dB	**9.5 dB**
Ouput Port Arrangements (△: in, •: out)	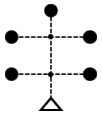	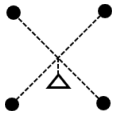	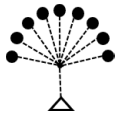	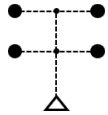	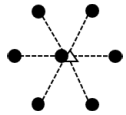

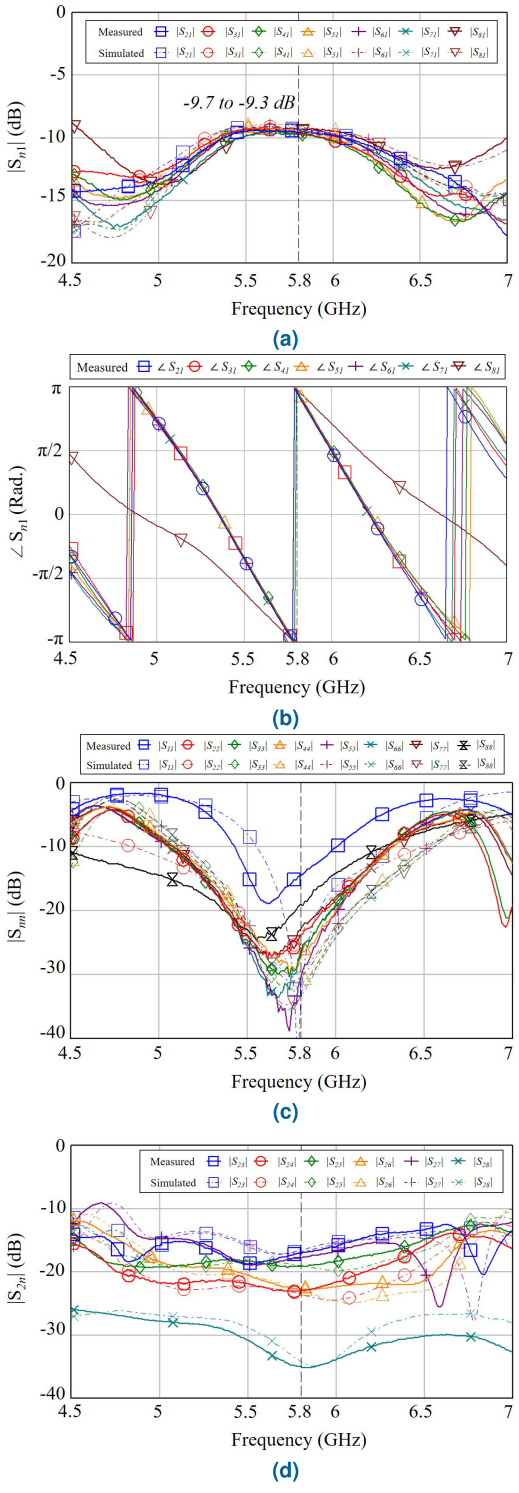

FIGURE 15. (a) Insertion loss, (b) Phase delay (c) Reflection and (d) Isolation between each port.

The comparison indicators include the number of ports, output port arrangement, substrate structure, operating frequency (BW) and insertion loss. To the best of our knowledge, the proposed divider is the only 7-way divider for the honeycomb structure, with an even power distribution and isolation value suitable for use as an *n*-way divider.

IV. CONCLUSION

In this paper, a new 7-way RF divider for a hexagonal honeycomb structure is presented. The proposed divider comprises a 6:1 unequal Wilkinson divider and a 6-way scattering structure divider implemented in a back-to-back microstrip line structure with a common ground. A coupled line is used to replace the high impedance transmission line in the uneven Wilkinson divider, which is difficult to fabricate with the conventional microstrip line. To verify the proposed design, a divider was designed and implemented with a center frequency of 5.8 GHz. The simulated and measured results showed that the divider can distribute power to seven honeycomb output ports with equal power and a phase difference of less than 4.7°. The fabricated divider works properly, and the proposed design scheme is expected to be used in RF systems involving hexagonal honeycomb structures.

REFERENCES

[1] W. Hong, K.-H. Baek, Y. Lee, Y. Kim, and S.-T. Ko, "Study and prototyping of practically large-scale mmWave antenna systems for 5G cellular devices," *IEEE Commun. Mag.*, vol. 52, no. 9, pp. 63–69, Sep. 2014.

[2] J.-Y. Lu, H.-J. Chang, and K.-L. Wong, "10-antenna array in the smartphone for the 3.6-GHz MIMO operation," in *Proc. IEEE Int. Symp. Antennas Propag. USNC/URSI Nat. Radio Sci. Meeting*, Vancouver, BC, Canada, Jul. 2015, pp. 1220–1221.

[3] H.-Y. Zhang, F.-S. Zhang, F. Zhang, F.-K. Sun, and G.-J. Xie, "High-power array antenna based on phase-adjustable array element for wireless power transmission," *IEEE Antennas Wireless Propag. Lett.*, vol. 16, pp. 2249–2253, 2017.

[4] R. J. Mailloux, "Pattern Synthesis for Linear and Planar Array," in *Phased Array Antenna Handbook*. New York, NY, USA: Artech House, 1994, pp. 109–180.

[5] Y. Wu, Y. Liu, Q. Xue, S. Li, and C. Yu, "Analytical design method of multiway dual-band planar power dividers with arbitrary power division," *IEEE Trans. Microw. Theory Techn.*, vol. 58, no. 12, pp. 3832–3841, Dec. 2010.

[6] H. Oraizi and S. A. Ayati, "Optimum design of a novel N-way planar power divider/combiner with impedance matching," *IET Microw., Antennas Propag.*, vol. 6, no. 4, pp. 418–425, 2012.

[7] E. J. Wilkinson, "An *N*-way hybrid power divider," *IRE Trans. Microw. Theory Techn.*, vol. 8, no. 1, pp. 116–118, Jan. 1960.

[8] J. R. Montejo-Garai, J. A. Ruiz-Cruz, and J. M. Rebollar, "A 10-way power divider based on a transducer and a radial junction operating in the circular TM01 mode," *IEEE Access*, vol. 7, pp. 127353–127361, 2019.

[9] T. Yu, J.-H. Tsai, and Y. Chang, "A radial four-way power divider with the proposed isolation network," *IEEE Microw. Wireless Compon. Lett.*, vol. 28, no. 3, pp. 194–196, Mar. 2018.

[10] B. Wu, Y. Zhang, Y. Zhao, W. Zhang, and L. He, "Compact nine-way power divider with omnidirectional resistor based on graphene flake," *IEEE Microw. Wireless Compon. Lett.*, vol. 28, no. 9, pp. 762–764, Sep. 2018.

[11] G. Li, K. Song, F. Zhang, and Yu. Zhu, "Novel four-way multilayer SIW power divider with slot coupling structure," *IEEE Microw. Wireless Compon. Lett.*, vol. 25, no. 12, pp. 799–801, Dec. 2015.

[12] D. M. Pozar, *Microwave Engineering*, 2nd ed. New York, NY, USA: Wiley, 1998, pp. 318–323.

[13] D. S. Beyragh, S. Abnavi, and S. R. Motahari, "Implementation of N-way Gysel combiners using back to back microstrip structure," in *Proc. IEEE Int. Conf. Ultra-Wideband*, Nanjing, China, Sep. 2010, pp. 1–4.

[14] M. Steer, *Microwave and RF Design: A Systems Approach*, Raleigh, NC, USA: SciTech, 2010, pp. 221–230.

[15] J.-S. Lim, S.-W. Lee, C.-S. Kim, J.-S. Park, D. Ahn, and S. Nam, "A 4.1 unequal Wilkinson power divider," *IEEE Microw. Wireless Compon. Lett.*, vol. 11, no. 3, pp. 124–126, Mar. 2001.

[16] S. Oh, J.-J. Koo, M.-S. Hwang, C. Park, Y.-C. Jeong, J.-S. Lim, K.-S. Choi, and D. Ahn, "An unequal wilkinson power divider with variable dividing ratio," in *IEEE MTT-S Int. Microw. Symp. Dig.*, Honolulu, HI, USA, Jun. 2007, pp. 411–414.

[17] C.-P. Chang, C.-C. Su, S.-H. Hung, Y.-H. Wang, and J.-H. Chen, "A 6:1 unequal Wilkinson power divider with EBG CPW," *Prog. Electromagn. Res. Lett.*, vol. 8, pp. 151–159, 2009.
[18] Y.-J. Ko, J.-Y. Park, and J.-U. Bu, "Fully integrated unequal wilkinson power divider with EBG CPW," *IEEE Microw. Wireless Compon. Lett.*, vol. 13, no. 7, pp. 276–278, Jul. 2003.
[19] S. Akhtarzad, T. R. Rowbotham, and P. B. Johns, "The design of coupled microstrip lines," *IEEE Trans. Microw. Theory Techn.*, vol. 23, no. 6, pp. 486–492, Jun. 1975.
[20] H.-R. Ahn and B.-M. Kim, "Equivalent transmission-line sections for very high impedances and their application to branch-line hybrids with very weak coupling power," *J. Electromagn. Eng. Sci.*, vol. 9, no. 2, pp. 85–97, Jun. 2009.
[21] R. Mongia, I. Bhal, and P. Bhartia, *RF and Microwave Coupled-Line Circuits*. Norwood, MA, USA: Artech House, 1999, p. 190.
[22] E. Laermans, J. De Geest, D. De Zutter, F. Olyslager, S. Sercu, and D. Morlion, "Modeling complex via hole structures," *IEEE Trans. Adv. Packag.*, vol. 25, no. 2, pp. 206–214, May 2002.

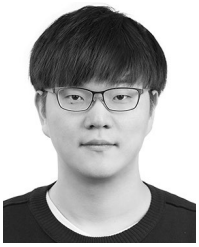

EUIBUM LEE (Student Member, IEEE) received the B.E. and M.S. degrees in electronic engineering from Konkuk University, Seoul, South Korea, in 2018 and 2020, respectively. His current research interests include wireless power transfer systems and RF circuit design.

HYUNCHUL KU (Member, IEEE) received the B.S. and M.S. degrees in electrical engineering from Seoul National University, Seoul, South Korea, in 1995 and 1997, respectively, and the Ph.D. degree in electrical and computer engineering from the Georgia Institute of Technology, Atlanta, GA, USA, in 2003. From 1997 to 1999, he worked at the Wireless Communication Research Center, KT, Seoul. From 2004 to 2005, he was employed at Research and Development Laboratory, Mobile Communication Division, Samsung Electronics, Suwon, South Korea. Since 2005, he has been with Konkuk University as a Professor. His research interests include digital RF systems, RF power amplifier, RF front-end design, and wireless power transfer systems.